Are There π^* Shape Resonances in Electron Scattering from Phosphate Groups?

Paul D. Burrow,*,† Gordon A. Gallup,† and Alberto Modelli‡

Department of Physics and Astronomy, University of Nebraska-Lincoln, Lincoln, Nebraska 68588-0111, Dipartimento di Chimica "G. Ciamician", Universitá di Bologna, 40126 Bologna, Italy, and Centro Interdipartimentale di Ricerca in Scienze Ambientali, Universitá di Bologna, 48100 Ravenna, Italy

Received: November 15, 2007; In Final Form: February 11, 2008

The temporary anion states of trimethyl phosphate and several compounds bearing the P═O group were explored using electron transmission spectroscopy and ab initio calculations to determine if these states have the characteristics of the π^* resonances usually associated with multiple bonds. No evidence was found for this in $(CH_3O)_3PO$ and, by extension, we do not expect them to appear in the phosphate group of DNA. Cl_3PO, however, does display such characteristics to some extent, and we show that they arise from the spatial properties of the σ^* (P−Cl) orbitals rather than from multiple PO bonding. A novel computational means to explore effects due to the relative size of a molecular orbital and that of the angular momentum barrier responsible for confining the additional electron is presented.

I. Introduction

To aid our understanding of bond-breaking in DNA induced by the formation of temporary negative ion states,[1,2] it is useful to study these processes in smaller subunits of DNA or in close surrogates for these moieties. In contrast to the DNA bases, in which resonances in the total scattering cross section associated with temporary occupation of the low-lying π^* orbitals have been observed[3] using electron transmission spectroscopy (ETS),[4] the empty orbitals of the phosphate and sugar groups are more problematic, and the role they play in bond-breaking, either by direct electron attachment or by transfer of an electron from elsewhere, is still the subject of active research. In the present work we focus on the phosphate group, see Scheme 1, as modeled by trimethyl phosphate (II), and other compounds bearing the PO bond usually drawn as P═O. In particular, we discuss the characteristics of temporary negative ion states that may be localized on the P═O portion of the molecule.

The properties of temporary negative ion states created by occupation of the normally empty π^* orbitals associated with C═C and C═O double bonds in compounds such as ethylene or formaldehyde, for example, or in more complex molecules made up of such groups, have been well documented. Conventionally, such states are described as "shape" resonances, reflecting the fact that the impinging electron is temporarily bound by the shape of the potential it encounters. They appear prominently as resonances in the total scattering cross sections[5] as observed by ETS, as well as in cross sections for excitation of vibrational modes.[6] An expansion in spherical harmonics of the π^* virtual orbital wave function of ethylene, for example, reveals angular momentum components $l \geq 2$ denoting a high angular momentum barrier and thus a relatively long resonance lifetime. Furthermore, because such a double bond will not be broken by addition of a single antibonding π^* electron, the anionic potential energy surface along the C═C stretch will have a minimum. Even in molecules with lower symmetry, such as H_2C═O, the anion lifetime is sufficient to display pronounced structure in the total scattering cross section arising from nuclear motion of the temporary anion along the double-bond stretching coordinate.[7]

SCHEME 1: Structural Formulas of Trimethyl Phosphite (I), Trimethyl Phosphate (II), Dimethyl Methylphosphonate (III), Dimethyl Acetylmethylphosphonate (IV), and Phosphoryl Chloride (V)

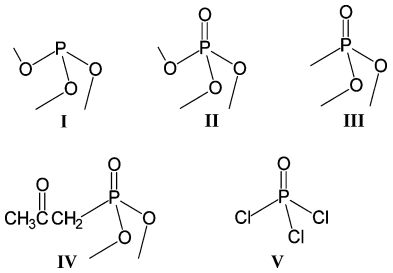

Because the phosphate group in DNA is normally pictured with a P═O bond, it is attractive to assume that a corresponding, normally empty, π^* orbital exists locally on this group. A number of authors have referred to such a π^* resonance, including a theoretical study of bond-breaking in sugar-phosphates at electron energies below 3 eV by Berdys et al.,[8] experimental studies of oligonucleotide tetramers on surfaces by Zheng et al.,[9] anion desorption studies from thin films of sodium dihydrogen phosphate by Pan and Sanche,[10] and gas-phase dissociative electron attachment (DEA) measurements of dibutylphosphate by Koenig et al.[11] The focus of the present work is to determine whether the properties of the temporary anion states of the phosphate group are similar in any way to those of the "traditional" π^* resonances mentioned earlier. Indeed, if such a long-lived resonance existed in the phosphate group, its properties should greatly influence direct electron attachment to the phosphate group, as well as acting as an efficient intermediary in transferring electrons from one portion of the molecule to another.

The representation of the PO bond in tertiary phosphine oxides, R_3PO, has been the subject of a great deal of discussion

* Corresponding author. Phone: (402) 472-2419. Fax: (402) 472-2879. E-mail: pburrow1@unl.edu.
† University of Nebraska-Lincoln.
‡ Universitá di Bologna.

10.1021/jp7109143 CCC: $40.75 © 2008 American Chemical Society
Published on Web 03/27/2008

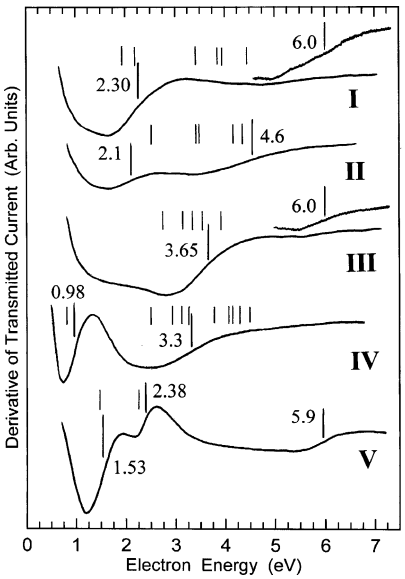

Figure 1. Derivative with respect to energy of transmitted electron current as a function of electron energy in compounds I−V. Long vertical lines indicate the energies of the experimental VAEs. The short vertical lines show the locations of predicted VAEs (scaled VOEs) determined from calculations discussed in the text.

and controversy. As described in a 1994 review by Gilheany,[12] a variety of structures have been invoked including $R_3P{=}O$, $R_3P^+-O^-$, "partial" triple bonds, formal triple bonds, and various resonance mixtures of these structures. In the intervening years, more sophisticated calculations have been possible, and in a recent atoms-in-molecules (AIM) study by Chesnut,[13] he concludes that the structure is best pictured as $R_3P^+-O^-$, comprised of one highly polarized σ bond and strong back-bonding of the oxygen π orbitals. If the normally accepted P═O double bond in HPO is taken as a reference bond order of 2.0, then the phosphoryl bond order in R_3PO is reported to be about 1.3. Finally, Chesnut concludes that the high degree of back-bonding provides for the stronger-than-single-bond character and short bond distance in R_3PO.

In the present work we report ETS studies of $(CH_3O)_3PO$ and related compounds (I, III−V) together with molecular orbital calculations to shed some light on the nature of the low-lying anion states of these compounds. Rather than deal with complex issues of classifying the PO bond, we take a more pragmatic view and search for the properties of the orbitals and the temporary anion structure in the electron scattering cross sections that might be characteristic of the presence of multiple bonds, regardless of their labeling.

II. Experimental Results

The ET spectra of five phosphorus compounds are presented in Figure 1, in which is plotted the derivative with respect to the energy of the electron current transmitted through a gas cell as a function of energy. The ET apparatus is in the format devised by Sanche and Schulz[4] and has been described elsewhere.[14] The long vertical lines, and their associated energies, indicate the midpoints of the minima and maxima in the derivative signals that we associate with the vertical attachment energies (VAEs) of the temporary anion states and the peaks in the total electron scattering cross section. The electron beam resolution was about 50 meV (fwhm). The energy scales were calibrated with reference to the $(1s^12s^2)^2S$ anion state of He. The estimated accuracy of the measured VAEs is ±0.05 or ±0.1 eV, depending on the number of decimal digits reported. All samples were commercially available and sufficiently volatile to give the required vapor pressure without heating the inlet system and collision chamber ($T\sim$ 40 °C).

TABLE 1: Virtual Orbital Energies and Scaled Orbital Energies Computed with DFT (B3LYP/6-31G(d)) and HF (6-31G(d)) Methods (All Energies in eV)

$(CH_3O)_3P$				
orbital	VOE(DFT)	scaled VOE[a]	VOE(HF)	scaled VOE[b]
LUMO	0.945	1.97	5.149	1.91
LUMO+1	1.220	2.19	5.409	2.11
LUMO+2	2.705	3.39	6.937	3.26
LUMO+3	3.243	3.82	7.453	3.64
LUMO+4	3.434	3.98	7.573	3.73
LUMO+5	3.987	4.42	8.434	4.38
$(CH_3O)_3PO$				
orbital				
LUMO (*a*)	1.571	2.48	6.129	2.65
LUMO+1,2 (*e*)	2.707	3.39	6.902	3.23
LUMO+3 (*a*)	2.735	3.41	7.249	3.49
LUMO+4,5 (*e*)	3.617	4.12	8.183	4.19
LUMO+6 (*a*)	3.825	4.29	8.299	4.28
$CH_3P(O)(CH_3O)_2$				
orbital				
LUMO	1.891	2.73	5.911	2.48
LUMO+1	2.384	3.13	6.805	3.16
LUMO+2	2.600	3.31	7.009	3.31
LUMO+3	2.874	3.53	7.123	3.40
LUMO+4	3.349	3.91	7.438	3.63
$(OCH_3)_2P(O)(CH_2COCH_3)$				
orbital				
LUMO	−0.543	0.77		
LUMO+1	1.627	2.52		
LUMO+2	2.147	2.94		
LUMO+3	2.344	3.10		
LUMO+4	2.558	3.27		
LUMO+5	3.203	3.79		
LUMO+6	3.524	4.05		
LUMO+7	3.617	4.12		
LUMO+8	3.801	4.27		
LUMO+9	4.058	4.48		

[a] π^* DFT scaling from ref 22. VAE = 0.80543VOE + 1.21099. [b] π^* HF scaling from ref 21. VAE = 0.753VOE −1.968.

For purposes of comparison, of the five compounds shown in Scheme 1, one, trimethyl phosphite (I), does not contain the PO bond that is the focus of our study. Another compound, dimethyl acetylmethylphosphonate $CH_3COCH_2P(O)(OCH_3)_2$ (IV), contains an unsaturated C═O bond, giving rise to the expected π^* resonance lying at 0.98 eV,[15] where we use the π^* symmetry designation in a local sense. This π^*_{CO} resonance is the lowest-lying feature observed in the spectra of the compounds considered (we recall here that formation of stable anion states cannot be detected with the ETS technique).

Although the experimental conditions under which the ETS data are taken are approximately the same for all of the compounds, we note that the structure appearing in the data for $(CH_3O)_3PO$ is considerably weaker than that in all the other compounds, including $(CH_3O)_3P$, which does not contain the PO bond. Alternatively, the two low-lying structures in Cl_3PO are strong and relatively narrow in width. At this point, we would conclude that there is little experimental evidence in trimethyl phosphate for a long-lived resonance associated with the PO bond, whereas in Cl_3PO the possibility for such anion states cannot be rejected.

TABLE 2: Virtual Orbital Energies and π^* and σ^* Scaled Orbital Energies Computed with DFT (B3LYP/6-31G(d)) and HF (6-31G(d)) Methods in Cl_3PO (All Energies in eV)

	Cl_3PO					
orbital	VOE(DFT)	π^* scaled VOE[a]	σ^* scaled VOE[c]	VOE(HF)	π^* scaled VOE[b]	σ^* scaled VOE[d]
LUMO (*a*)	−2.854	−1.09	−0.71	1.911	−0.53	−0.83
LUMO+1,2 (*e*)	−0.145	1.09	1.49	4.617	1.51	1.61
LUMO+3 (*a*)	0.761	1.82	2.23	5.068	1.85	2.01
LUMO+4 (*a*)	6.109	6.13	6.57	10.072	5.62	6.52
LUMO+5,6 (*e*)	6.280	6.27	6.70	10.504	5.94	6.90

[a] π^* DFT scaling from ref 22. VAE = 0.80543VOE + 1.21099. [b] π^* HF scaling from ref 21. VAE = 0.753VOE − 1.968. [c] σ^* DFT scaling, present work. VAE = 0.8111VOE + 1.6097. [d] σ^* HF scaling from ref 25. VAE = 0.90VOE − 2.55.

III. Properties of Unfilled Molecular Orbitals

(a) Energy Considerations. To bolster our discussion, we have carried out calculations of the virtual orbitals of several of the compounds shown in Figure 1 and others that might illuminate our understanding. These were carried out using both HF ab initio methods as well as DFT with the B3LYP functional. Both approaches used geometry optimization and electronic structure computed at the 6-31G(d) basis set level.[16,17] Only the most stable conformer of each compound is considered further. As is well understood, the virtual orbital energies (VOEs) from Koopmans' Theorem[18] do not give the correct absolute energies of the resonances associated with electron occupation of the given virtual orbitals; however, their relative ordering and separations are meaningful. Consequently, it is useful to empirically scale the VOEs to measured VAEs in related molecules and use this correlation to predict the locations of temporary anion states more accurately. Such scalings using HF VOEs have been carried out for π^* resonances in numerous unsaturated compounds.[19−21] More recently, a π^* scaling for unsaturated compounds using B3LYP/6-31G(d) calculations has also been reported.[22]

Scalings for resonances associated with saturated bonds are generally not available because of the difficulty of observing σ^* resonances in molecules with light elements.[23] However, in a study of permethylated group 14 dimers,[24] good linear correlations have been found between σ^* VEAs and the corresponding VOEs obtained with different methods. Nevertheless, it has been pointed out that caution is needed in the application of these scalings to systems where the molecular structures or the nature of the σ^* MOs are different. A scaling for the σ^* (C−Cl) resonances in mono- and polychloroalkanes has been presented using HF calculations.[25] In this work we also present in Appendix A the scaling for these same σ^* (C−Cl) resonances based on DFT calculations.

Unfortunately, none of these scalings have been made using ETS results in phosphorus-bearing molecules similar to the compounds in Figure 1, so their application to the present data is less reliable. Table 1 lists the VOEs and π^*-scaled VOEs for $(CH_3O)_3P$, $(CH_3O)_3PO$, $CH_3P(O)(OCH_3)_2$, and $(OCH_3)_2P(O)(CH_2COCH_3)$. The HF[21] and DFT[22] scaled VOEs are in close agreement for the predicted anion state energies, with an average difference in energy (magnitude) of 0.12 eV for the empty orbitals listed. Although this agreement stems in part from the limited range of orbital energies involved, there is nothing to suggest one approach over the other and we have chosen to use the DFT π^*-scaled VO energies shown as short vertical lines in Figure 1 to compare with experiment for compounds I−IV.

The HF and DFT π^* scalings fare less well in Cl_3PO as shown in Table 2. It seems reasonable to select a scaling more directed to the presence of Cl atoms for this compound. Thus, we have included the HF scaling of ref 25 and the DFT scaling presented in Appendix A for σ^* (C−Cl) resonances in chloroalkanes. Both produce excellent agreement with experiment for the lowest lying resonances, keeping in mind that the feature at 2.38 eV is overlapped by the lowest resonance and is thus an upper bound. In the geometry of the neutral molecule, the anionic ground state of Cl_3PO is predicted to be stable by 0.7−0.8 eV, consistent with an adiabatic electron affinity of 1.4 eV as found experimentally.[26] The short lines for this compound in Figure 1 correspond to the DFT values.

The scaled VOEs provide a very good match for the sharpest structures seen in Figure 1. For example, in Cl_3PO (**V**) the scaled VOEs of the first *e* and second *a* orbitals give excellent agreement with the ETS results. The relatively narrow width of the resonance displayed at 5.9 eV indicates a sizable core-excited character, obviously not accounted for by KT calculations. The cross section peaks associated with σ^* MOs are usually small and broad, and the substantial overlapping makes a unique attribution problematic. The two lowest temporary anion states of $(CH_3O)_3P$ (**I**) are each in good agreement with the structure at 2.38 eV. The VOEs were determined from the lowest conformer, which does not have C_3 symmetry. (In the C_3 conformer, the lowest empty orbital is the doubly degenerate *e* pair and their scaled VOE lies at 2.05 eV.)

In $CH_3P(O)(CH_3O)_2$ (**III**) the predicted anion states range from 2.73 to 3.91 eV, in general agreement with the broad ETS feature at 3.7 eV. These states, as well as those in the C═O bearing compound, are destabilized relative to those of $(CH_3O)_3P$ because of the absence of the third CH_3O group and its inductive effect, as well as the replacement of a σ^* (P−O) orbital with a higher-lying σ^* (P−C) orbital.

In $(CH_3O)_3PO$ (**II**), only the anion state associated with the lowest *a* orbital is in approximate agreement with experiment for the feature at 2.11 eV. The second *e* orbital pair could account for the weak broad resonance at 4.6 eV.

(b) Spatial Characteristics. We next examine the spatial characteristics of the lower empty orbitals of several of the P═O bearing compounds, namely, $(CH_3O)_3PO$, Cl_3PO and a compound for which we do not have ETS data, $HOP(O)(CH_3O)_2$. The latter is closer to the form of the phosphate group in DNA but with the O^- protonated, as assumed in some theoretical treatments.[27] We begin with the lowest unoccupied molecular orbitals (LUMOs) shown in Figure 2, including also LUMO+1 of $HOP(O)(CH_3O)_2$. In each case the orbital is drawn with the P═O group pointed downward. All of these orbitals are of the most symmetric type allowed, and none produce anions with π^* character. Nevertheless, we include them for completeness.

The LUMO of $(CH_3O)_3PO$ shows considerable delocalization over the entire molecule. In contrast, the LUMO of the more compact Cl_3PO molecule is clearly comprised of the σ^* (P−

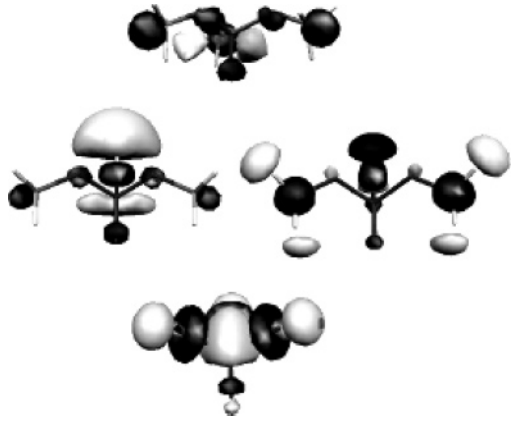

Figure 2. Virtual molecular orbitals plotted with the P═O bond pointed downward. Top, $(CH_3O)_3PO$ LUMO (*a*); middle left, $HOP(O)(CH_3O)_2$ LUMO (*a′*); middle right, $HOP(O)(CH_3O)_2$ LUMO+1 (*a′*); bottom, Cl_3PO LUMO (a_1).

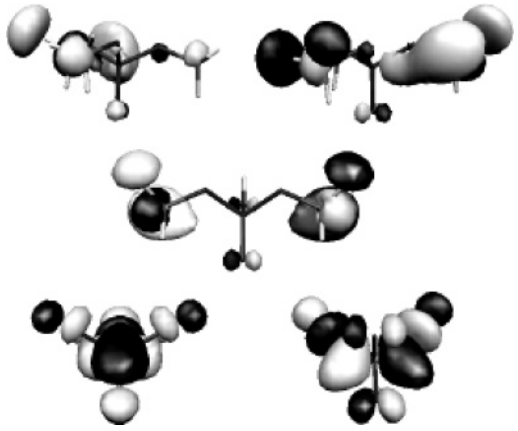

Figure 3. As in Figure 2: top left, $(CH_3O)_3PO$ LUMO+1 (e_x); top right, $(CH_3O)_3PO$ LUMO+2 (e_y); middle, $HOP(O)(CH_3O)_2$ LUMO+2 (*a″*); bottom left, Cl_3PO LUMO+1 (e_x); bottom right, Cl_3PO LUMO+2 (e_y).

Cl) orbitals. As noted earlier, occupation of this orbital in Cl_3PO leads to a stable anion state.

The middle row of Figure 2 shows the effect of replacing a methyl group on $(CH_3O)_3PO$ with a hydrogen atom. The LUMO, and LUMO+1 to a lesser extent, are now dominated by the σ^* (OH) orbital. Hydroxy groups are often present in experimental studies of *surrogates* of the deoxyribose and phosphate groups of DNA. In theoretical treatments they may appear from termination of broken C−O bonds and from protonation of $P-O^-$ of the DNA phosphate group.[27] Figure 2 illustrates the substantial changes in the lower orbitals that are a consequence of the low energy of the σ^* (OH) group compared with σ^* orbitals of other bonds. As discussed elsewhere,[28] their presence leads to an enhancement of the DEA cross section.

In the theoretical treatment of a sugar−phosphate−sugar complex by Berdys et al. ,[8] the lowest lying anion state is labeled π^* and is largely confined to the phosphate group and the neighboring carbon atoms (shown in their Figure 8). A substantial portion of the wave function lies on the OH group attached to the phosphorus atom. The present work suggests that this orbital is the analog of the LUMO (a′) of $HOP(O)(CH_3O)_2$ shown in the middle of Figure 2. As we argue in this work, this orbital has none of the characteristics of a canonical π^* resonance.

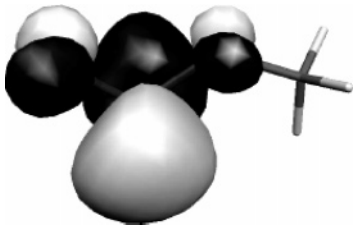

Figure 4. LUMO of CH_3OPO.

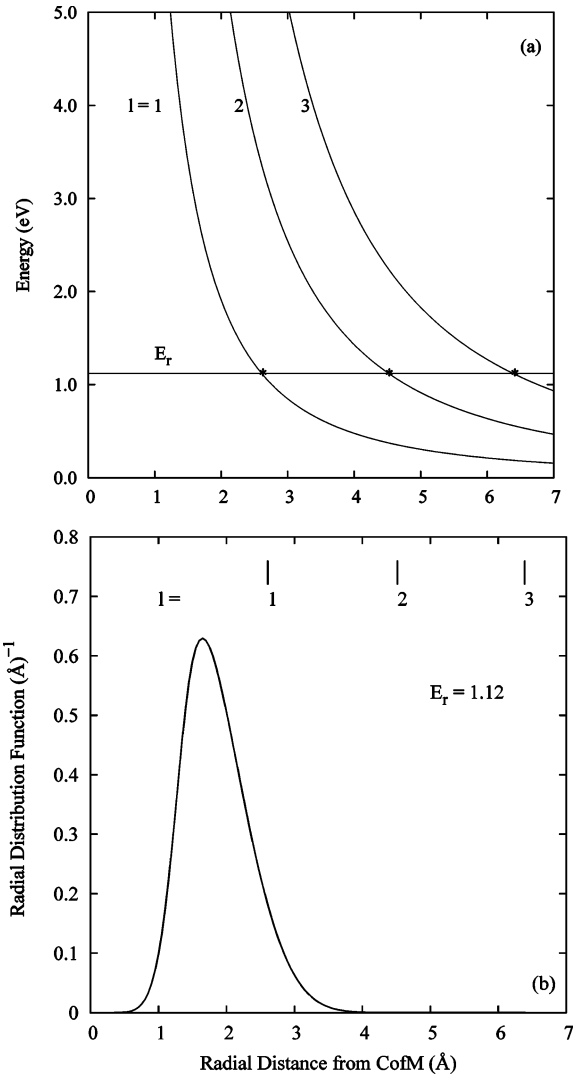

Figure 5. (a) Effective potential energy arising from the angular momentum of the impinging electron for $l = 1$, 2, and 3 as a function of the radial distance from the center of mass of a molecule. The horizontal line and dots indicate the radial distances where a resonance energy of 1.12 eV equals the potential energy from the angular momentum. (b) The radial distribution function of the LUMO of benzene plotted as a function of the radial distance from the center of mass.

In Figure 3 we plot the *e* (LUMO+1,2) pairs of $(CH_3O)_3PO$ and Cl_3PO and the corresponding *a″* (LUMO+2) of $HOP(O)(CH_3O)_2$. Our objective here is to search for "π^*-like" lobes in these orbitals. To assist in this, we show for comparison in Figure 4 the LUMO of CH_3OPO, a compound in which it is generally agreed that a double bond and its corresponding antibonding orbital exist. In this compound the π^* orbital is delocalized also on the neighboring O atom, resembling an allylic LUMO. In our opinion, the orbitals of the upper two compounds of Figure 3 do not exhibit such an orbital charac-

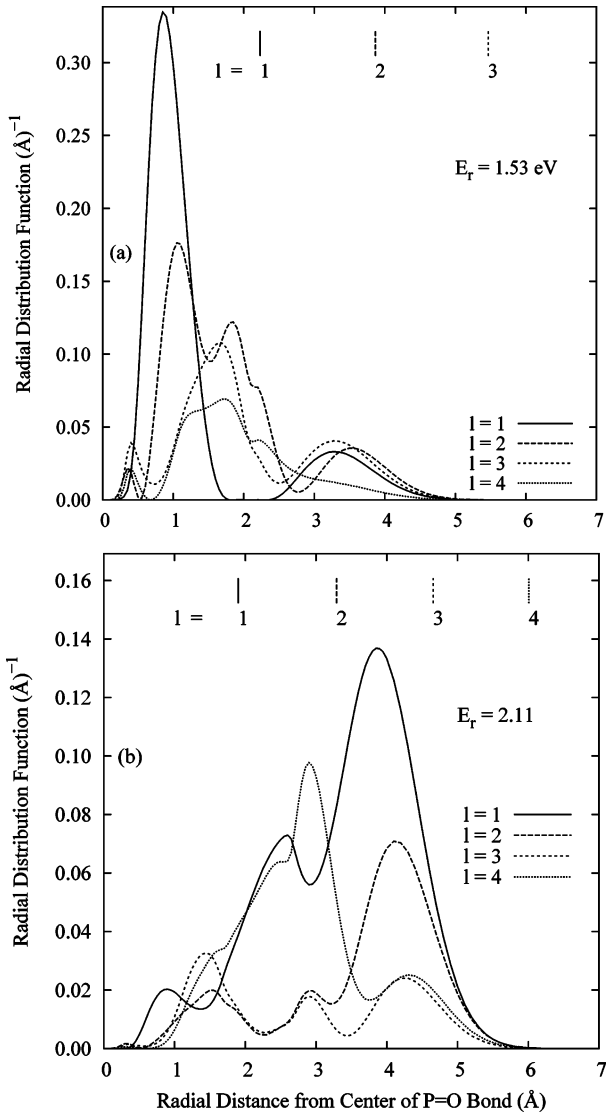

Figure 6. (a) Radial distribution function of the LUMO+1 (e_x) of Cl_3PO as a function of the radial distance from the center of the P═O bond. The resonance energy is taken to be 1.53 eV, and the vertical lines indicate the distances at which this energy equals the potential energy associated with the angular momentum for $l = 1$, 2, and 3. (b) As in panel a for the LUMO+1 (e_x) of $(CH_3O)_3PO$ and a resonance energy of 2.11 eV.

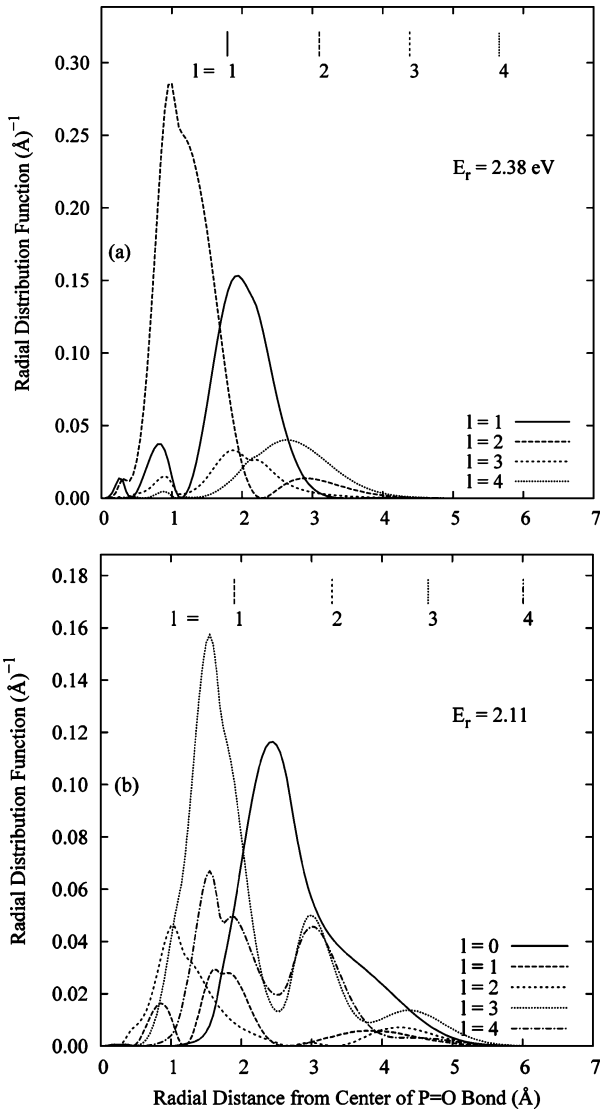

Figure 7. (a) As in Figure 6 for the LUMO+3 (a_1) of Cl_3PO at a resonance energy of 2.38 eV. (b) As in Figure 6 for the LUMO (a_1) of $(CH_3O)_3PO$ at a resonance energy of 2.11 eV.

teristic to any reasonable extent. Because of its symmetry, the clearest view is perhaps that of the a'' orbital in HOP(O)-$(CH_3O)_2$. In contrast, a volume of space around PO in the e orbitals of Cl_3PO does have this property. It appears that the smaller size of Cl_3PO and the lower-lying e orbitals give rise to resonances that have more similarity to π^* orbitals, whereas in $(CH_3O)_3PO$ the orbitals are much more extended and removed from the P═O portion of the molecule.

(c) Expansions in Spherical Harmonics. In simple spherical systems the widths, proportional to the inverse of the lifetimes, of shape resonances are well known to be associated with electron tunneling through an angular momentum barrier. Thus, in these systems, resonances with s symmetry do not occur. In molecules, however, the barrier can be considered a mixture of terms with different l values, and the total lifetime depends upon an average that reflects how these various terms allow the electron wave function to "leak out" into the continuum. Unlike the case with atoms, molecules may show resonant behavior with states of symmetry types where the leading l value is 0.

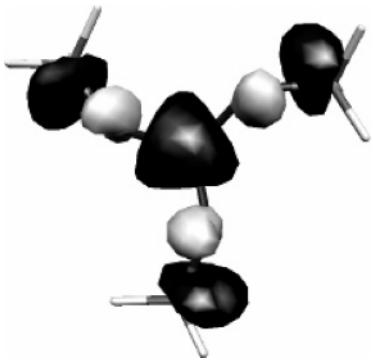

Figure 8. LUMO + 3 (a) of $(CH_3O)_3PO$, the lowest normally empty orbital showing strongly antibonding character at the C−O bonds. The P═O bond is oriented into the paper.

To make our earlier discussion more quantitative, we have calculated the spherical harmonic expansions of several of the Koopmans' Theorem (KT) quasi-bound state functions that occur in the molecules discussed here. Thus, if we represent a resonant wave function as $\varphi(r)$, then we may write

$$\varphi(\vec{r}) = \sum_{lm} f_{lm}(r)\, Y_{lm}(\theta,\phi) \quad (1)$$

For our purposes, we approximate $\varphi(\vec{r})$ in the region of the molecule with the quasi-bound state of the resonance, which is a normalizable function and can be used to produce population numbers. Thus, if an expansion like that of eq 1 is applied to these, then we define the population associated with l to be

$$P_l = \sum_m \int_0^\infty |f_{lm}|^2 r^2\, dr \quad (2)$$

and

$$\sum_l P_l = 1 \quad (3)$$

For use later, we also define the lth radial distribution function as

$$p_l(r) = \sum_m |r\, f_{lm}(r)|^2 \quad (4)$$

We point out that these functions depend upon the point in the molecule about which the expansion is determined. A quantum mechanically correct treatment of electron scattering from freely rotating molecules suggests that the center of mass is the appropriate point to use for such a spherical harmonic expansion because the separation of translation and rotation requires it. However, our objective here is to probe the spatial characteristics of the wave function in the neighborhood of the PO bond, and we choose to do the expansion around the midpoint of this bond. The dominant population numbers in such expansions give an indication of the relative contributions of the various angular momentum quantum numbers making up the orbital wave functions in the locality of the expansion point. In the π^* orbital of ethylene, for example, $l = 2$ is the leading and dominant term in such an expansion. In H_2CO, however, both $l = 1$ and 2 will be present because of the difference in charge on the atoms of the double bond.

Table 3 lists the calculated populations for $l = 0-5$ in the orbitals shown in Figure 3. Consistent with our inferences from the orbital plots, the LUMO+1 (e_x) orbital of Cl_3PO displays the largest $l = 2$ population of the three compounds. A substantial amount of $l = 1$ is present in all three cases.

The populations computed above have been integrated over the entire radial extent of the orbitals. In an atomic temporary anion state, the barrier produced by the angular momentum and the attractive screened-coulomb and polarization potentials are responsible for trapping the electron, and one expects the electron wave function to lie primarily inside the barrier. Because of the spatial extent of a molecule, the question arises whether the orbital wave function actually lies within the barrier or not. In other words, a delocalized orbital as in $(CH_3O)_3PO$ could have a substantial fraction of its orbital lying outside the barrier where it cannot contribute to the formation of a resonance, whereas in a smaller compound like Cl_3PO the orbital could be mostly contained within the barrier.

To explore this possibility, we plot in Figure 5a the effective potential energy (PE) associated with the angular momentum barriers for $l = 1-3$ as a function of the radial distance r from the center of mass of a test molecule, in this case, benzene. The horizontal line at $E_R = 1.12$ eV defines the experimental energy of the well-known $^2E_{2u}$ resonance.[29] The intersection of this line defines for each l a radial distance at which E_R is equal to the height of the angular momentum PE. For a resonance at E_R, the position of the barrier maximum should lie within this distance, and roughly speaking, we expect that the electron wave function will as well. An expansion in spherical harmonics of the e_{2u} orbital of benzene shows that the leading and dominant component is $l = 3$. In Figure 5b we plot the corresponding radial distribution function defined in eq 4 as a function of the distance from the center of mass. The three vertical lines marked 1, 2, and 3 indicate the radial distances at which the resonance energy equals the PE of the associated angular momentum barriers. The figure indicates that the radial distribution function indeed lies well within the barrier for $l = 3$ and, for the most part, even within that for $l = 1$. These properties likely account for the narrow width of this resonance.

TABLE 3: Relative Fraction of Each Indicated Virtual Orbital in Components of the Angular Momentum

	$(CH_3O)_3PO$	$(CH_3O)_2OHPO$	Cl_3PO
l	LUMO+1(e_x)	LUMO+2(a'')	LUMO+1(e_x)
0	0.000	0.000	0.000
1	0.281	0.318	0.259
2	0.118	0.054	0.243
3	0.066	0.048	0.164
4	0.161	0.196	0.109
5	0.168	0.070	0.041

TABLE 4: Relative Fraction of Each Indicated Virtual Orbital in Components of the Angular Momentum

	$(CH_3O)_3PO$	Cl_3PO
l	LUMO (a)	LUMO+3(a_1)
0	0.304	0.093
1	0.036	0.163
2	0.048	0.270
3	0.186	0.040
4	0.101	0.057
5	0.065	0.079

In Figure 6a and 6b we plot radial distribution functions for $l = 1-5$ as a function of the distance r from the center of the PO bond for the e orbitals in Cl_3PO and $(CH_3O)_3PO$, respectively. (Participation of $l = 0$ is forbidden by symmetry to contribute to these orbitals.) For the indicated experimental resonance energies, E_R, the vertical lines indicate for each l value the radial distance at which E_R equals the angular momentum PE as in Figure 5. For $(CH_3O)_3PO$ we assume that the e resonance energy lies at the experimental value (2.11 eV) given in Figure 1.

In Cl_3PO, the dominant components are for the key values $l = 1$ and 2 that should characterize a π^* orbital, and both lie inside the $l = 1$ distance and well within that for $l = 2$. In $(CH_3O)_3PO$, in contrast to Cl_3PO, one expects contributions to lie at much greater radial distances because of the larger size of this molecule. The maxima in both the $l = 1$ and $l = 2$ components are calculated to lie *outside* their respective barrier distances. The electron trapping that does occur may be a consequence of the $l = 3$ component, the second largest in $(CH_3O)_3PO$, which does lie within its barrier.

The results of these calculations again support the contention that the e orbital of $(CH_3O)_3PO$ does not possess π^* characteristics whereas that in Cl_3PO does. It should be noted that in the latter case these characteristics do not arise as a consequence of multiple bonding as in, say, ethylene, but rather from the positions of the P−Cl σ^* orbitals.

(d) Characteristics of Totally Symmetric Empty Orbitals. In Cl_3PO, occupation of the second empty orbital of a_1 symmetry (LUMO+3) also gives rise to a pronounced reso-

TABLE 5: Vertical Attachment Energies and Virtual Orbital Energies Computed by DFT (Energies in eV)

compound	VAE	VOE
chloroethane	2.41	0.752
1-chloropropane	2.4	0.718
1-chlorobutane	2.43	0.76
2-chloropropane	1.97	0.691
2-chlorobutane	2.05	0.725
tert-butychloride	1.86	0.546
2,2-dichloropropane	1.41	−0.294
1,1-dichloropropane	1.39	−0.272
1,1-dichloroethane	1.36	−0.331
dichloromethane	1.01	−0.434
1,1,1-trichloroethane	0.64	−1.228
trichloromethane	0.42	−1.353
1,1,1,2-tetrachloroethane	0.63	−1.446

nance, seen in Figure 1 near 2.38 eV. In this section we compare the properties of this totally symmetric orbital, in which $l = 0$ is permitted, with those of the LUMO of $(CH_3O)_3PO$, also totally symmetric. Table 4 shows the angular momentum components of these orbitals integrated over all radial distances (from the center of the P═O bond) as done in Table 3 for the resonances of *e* symmetry. There are two striking differences between the two compounds. In Cl_3PO, the a_1 orbital (LUMO+3) has its largest contribution in $l = 2$ and second largest in $l = 1$. In $(CH_3O)_3PO$ these contributions are almost negligible. Furthermore, the $l = 0$ contribution, which does not generate a barrier, is the largest observed in any of the present calculations.

We examine the radial distributions as a function of distance in Figure 7a (Cl_3PO) and 7b ($(CH_3O)_3PO$). Consistent with the data in Table 4, the $l = 2$ and $l = 1$ components of Cl_3PO are largest by a big margin and the maxima fall within the respective rough barrier distances. These properties appear sufficient to give rise to a pronounced resonance.

In Figure 7b we assume for our calculation that the LUMO of $(CH_3O)_3PO$ gives rise to the weak resonance at 2.11 eV. As in Table 4, the $l = 0$ component is quite large compared to the small contribution observed in Cl_3PO. This indicates that a substantial fraction of the wave function cannot be trapped and that the resonance must arise from the remaining $l = 3$ component that is well within its barrier. We suggest that the large component of $l = 0$ is responsible for the reduced resonance visibility, but this conclusion needs to be studied further with similar calculations in other molecular systems and comparison with experiment.

IV. C−O Antibonding Character in $(CH_3O)_3PO$

Finally, we consider briefly the lowest empty orbitals of $(CH_3O)_3PO$ and their properties with regard to antibonding character at the C−O bonds. Theoretical treatments of DNA strand-breaking by Simons and collaborators[27] indicate that the C−O bond of the phosphate-sugar link is the most likely to be broken by the presence of an electron, owing to the large electron affinity of the phosphate fragment. For computational simplicity, they modeled only a section of a DNA single strand containing a base, a sugar, and a phosphate group. Furthermore, the phosphate group was protonated and H atoms were added at the dangling bonds. As noted earlier, these low-lying σ^* (OH) orbitals tend to dominate the empty orbital spectrum.

Examination of the empty orbitals of $(CH_3O)_3PO$ shows that neither the LUMO (*a*) nor LUMO+1,2 (*e*) possesses C−O antibonding character. LUMO+3, the *second* empty orbital of *a* symmetry, appears to be the lowest lying orbital with this property, and this is illustrated in Figure 8 with the P═O bond perpendicular to the paper. Direct electron attachment into this

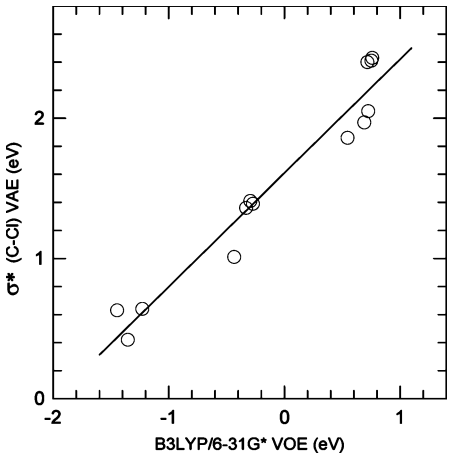

Figure 9. Measured VAEs as a function of calculated VOEs in a series of mono- and polychloroalkanes.

orbital, or more properly, the orbital most closely related to it in the actual DNA phosphate group, should be considered as a possible shape resonance mechanism for breaking the C−O bond. From the point of view of the treatment of the Simons' group, the coupling of this orbital to the π^* resonances of the base would be the most relevant to describe bond breaking by transfer of an electron initially attached to the base.

V. Conclusions

The properties of the temporary anion states of various P═O bearing compounds have been examined from several approaches including ETS measurements, molecular orbital plots, and an analysis of the empty orbitals in terms of spherical harmonic decompositions and their radial dependence. Excepting Cl_3PO, none of the compounds exhibit properties that suggest a local π^* orbital associated with the "nominal" PO double bond. In the case of Cl_3PO, these properties are present but arise from the wave function lobes associated with the σ^* (P−Cl) orbitals rather than from a multiple bond. Our results, therefore, are consistent with and augment past theoretical studies[13] of the filled orbitals of this group of compounds that suggest the "P═O" bond in these compounds is an abnormally short and strong single bond.

In terms of electron scattering from DNA, there is little reason therefore to expect or invoke a π^* resonance, *as traditionally understood*, that is resident on the phosphate group. This is also consistent with calculations by Winstead and McKoy[30] on the nucleotide deoxyadenosine monophosphate, and Tonzani and Greene[31] on H_3PO_4. Although the issue of a PO-based π^* orbital was not addressed specifically, the calculated integral elastic scattering cross sections showed no low-lying features that could be attributed to such a resonance. Regardless of its label, this resonance is not involved in the theoretical treatment of bond-breaking in DNA by Simons' group.[27]

In summary, it appears that the resonances attributed to the "π^*" orbital of the phosphates are short-lived and comprised of delocalized combinations of σ^* orbitals. Their role in DNA bond-breaking remains to be determined.

Appendix A

The measured VAEs of a series of mono- and polychloroalkanes are given in Table 5 below together with the VOEs computed by DFT at the B3LYP/6-31G(d) level. The temporary anion states are those associated with electron occupation of σ^*(C−Cl) orbitals. The VAEs are compiled in ref 25. A plot

of VAE versus VOE is shown in Figure 9, and a linear regression through the data yields VAE = 0.8111 VOE + 1.6097 in eV, and r sq. = 0.946.

Acknowledgment. A.M. thanks the Italian Ministero dell'Istruzione, dell'Università e della Ricerca for financial support.

References and Notes

(1) Boudaiffa, B.; Cloutier, P.; Hunting, D.; Huels, M. A.; Sanche, L. *Science* **2000**, *287*, 1658.
(2) Martin, F.; Burrow, P. D.; Cai, Z.; Cloutier, P.; Hunting, D.; Sanche, L. *Phys. Rev. Lett.* **2004**, *93*, 068101.
(3) Aflatooni, K.; Gallup, G. A.; Burrow, P. D. *J. Phys. Chem. A* **1998**, *102*, 6205.
(4) Sanche, L.; Schulz, G. J. *Phys. Rev. A* **1972**, *5*, 1672.
(5) See, for example, Jordan, K. D.; Burrow, P. D. *Chem. Rev*. **1987**, *87*, 557.
(6) For example, Walker, I. C.; Stamatovic, A.; Wong, S. F. *J. Chem. Phys*. **1978**, *69*, 5532.
(7) Burrow, P. D.; Michejda, J. A. *Chem. Phys. Lett.* **1976**, *42*, 223.
(8) Berdys, J.; Anusiewicz, I.; Skurski, P.; Simons, J. *J. Am. Chem. Soc*. **2004**, *126*, 6441.
(9) Zheng, Y.; Cloutier, P.; Hunting, D. J.; Sanche, L.; Wagner, J. R. *J. Am. Chem. Soc*. **2005**, *127*, 16592.
(10) Pan, X.; Sanche, L. *Chem. Phys. Lett.* **2006**, *421*, 404.
(11) Koenig, C.; Kopyra, J.; Bald, I.; Illenberger, E. *Phys. Rev. Lett.* **2006**, *97*, 018105.
(12) Gilheany, D. G. *Chem. Rev*. **1994**, *94*, 1339.
(13) Chesnut, D. B. *J. Phys. Chem. A* **2003**, *107*, 4307.
(14) Modelli, A.; Jones, D.; Distefano, G. *Chem. Phys. Lett.* **1982**, *86*, 434.
(15) (a) Van Veen, E. H.; Van Dijk, W. L.; Brongersma, H. H. *Chem. Phys*. **1976**, *16*, 337. (b) Jordan, K. D.; Burrow, P. D. *Acc. Chem. Res*. **1978**, *11*, 342.
(16) (a) Schmidt, M. W.; Baldridge, K. K.; Boatz, J. A.; Elbert, S. T.; Gordon, M. S.; Jensen, J. H.; Koseki, S.; Matsunaga, N.; Nguyen, K. A.; Su, S. J.; Windus, T. L.; Dupuis, M.; Montgomery, J. A. *Comput. Chem*. **1993**, *14*, 1347. (b) Granovsky, A. A. PC GAMESS version 7.0, http://classic.chem.msu.su/gran/gamess/index.html.
(17) Frisch, M. J.; Trucks, G. W.; Schlegel, H. B.; Scuseria, G. E.; Robb, M. A.; Cheeseman, J. R.; Montgomery, J. A., Jr.; Vreven, T.; Kudin, K. N.; Burant, J. C.; Millam, J. M.; Iyengar, S. S.; Tomasi, J.; Barone, V.; Mennucci, B.; Cossi, M.; Scalmani, G.; Rega, N.; Petersson, G. A.; Nakatsuji, H.; Hada, M.; Ehara, M.; Toyota, K.; Fukuda, R.; Hasegawa, J.; Ishida, M.; Nakajima, T.; Honda, Y.; Kitao, O.; Nakai, H.; Klene, M.; Li, X.; Knox, J. E.; Hratchian, H. P.; Cross, J. B.; Bakken, V.; Adamo, C.; Jaramillo, J.; Gomperts, R.; Stratmann, R. E.; Yazyev, O.; Austin, A. J.; Cammi, R.; Pomelli, C.; Ochterski, J. W.; Ayala, P. Y.; Morokuma, K.; Voth, G. A.; Salvador, P.; Dannenberg, J. J.; Zakrzewski, V. G.; Dapprich, S.; Daniels, A. D.; Strain, M. C.; Farkas, O.; Malick, D. K.; Rabuck, A. D.; Raghavachari, K.; Foresman, J. B.; Ortiz, J. V.; Cui, Q.; Baboul, A. G.; Clifford, S.; Cioslowski, J.; Stefanov, B. B.; Liu, G.; Liashenko, A.; Piskorz, P.; Komaromi, I.; Martin, R. L.; Fox, D. J.; Keith, T.; Al-Laham, M. A.; Peng, C. Y.; Nanayakkara, A.; Challacombe, M.; Gill, P. M. W.; Johnson, B.; Chen, W.; Wong, M. W.; Gonzalez, C.; Pople, J. A. *Gaussian 03*, revision C.02; Gaussian, Inc.: Wallingford, CT, 2004.
(18) Koopmans, T. *Physica* (*Amsterdam*) **1934**, *1*, 104.
(19) Chen, D.; Gallup, G. A. *J. Chem. Phys*. **1990**, *93*, 8893.
(20) Staley, S. W.; Strnad, J. T. *J. Phys. Chem*. **1994**, *98*, 161.
(21) Aflatooni, K.; Gallup, G. A.; Burrow, P. D. *J. Phys. Chem. A* **1998**, *102*, 6205. The scaling in the present work differs slightly from that in this reference because the earlier geometry optimization was carried out with the 3-21G basis set.
(22) Modelli, A. *Phys. Chem. Chem. Phys.* **2003**, *5*, 2923.
(23) Modelli, A. *Trends Chem. Phys. (Research Trends*) **1997**, *6*, 57.
(24) Modelli, A.; Szepes, L. *Chem. Phys*. **2003**, *286*, 165.
(25) Aflatooni, K.; Gallup, G. A.; Burrow, P. D. *J. Phys. Chem. A* **2000**, *104*, 7359.
(26) Mathur, B. P.; Rothe, E. W.; Tang, S. Y. *J. Chem. Phys*. **1976**, *65*, 565.
(27) Barrios, R.; Skurski, P.; Simons, J. *J. Phys. Chem B* **2002**, *106*, 7991.
(28) Aflatooni, K.; Scheer, A. M.; Burrow, P. D. *J. Chem. Phys*. **2006**, *125*, 054301.
(29) Sanche, L.; Schulz, G. J. *J. Chem. Phys.* **1973**, *58*, 479.
(30) Winstead, C.; McKoy, V. *J. Chem. Phys*. **2006**, *125*, 244302.
(31) Tonzani, S.; Greene, C. H. *J. Chem. Phys*. **2006**, *125*, 094504.